

Surface and core magnetic anisotropy in maghemite nanoparticles determined by pressure experiments

Y. Komorida,^{1,a)} M. Mito,¹ H. Deguchi,¹ S. Takagi,¹ A. Millán,² N. J. O. Silva,^{2,b)} and F. Palacio²

¹Faculty of Engineering, Kyushu Institute of Technology, Kitakyushu 804-8550, Japan

²Departamento de Física de la Materia Condensada, Facultad de Ciencias, Instituto de Ciencia de Materiales de Aragón, CSIC-Universidad de Zaragoza, 50009 Zaragoza, Spain

(Received 9 December 2008; accepted 18 February 2009; published online 19 May 2009)

In magnetic nanoparticles, anisotropy energy has extra contributions compared to that of the bulk counterparts, being the most relevant surface anisotropy. Here we use pressure to separate core from surface anisotropy in one system of maghemite nanoparticles dispersed in a polymer. The core anisotropy is $K_{\text{core}}=7.7 \times 10^5$ erg/cm³ while the surface anisotropy is $K_S=4.2 \times 10^{-2}$ erg/cm². This in-one-sample separation is possible due to changes in structurally ordered and disordered ratio, which induce changes in the average magnetic anisotropy energy. © 2009 American Institute of Physics. [DOI: 10.1063/1.3131782]

Nanoparticle properties often differ from those of the bulk material due to finite size and surface effects. However, it is not straightforward to separate these effects and to investigate the intrinsic origin of the changes associated to the reduction of size in each property separately. In the frame of magnetic nanoparticles, size dependent magnetic properties include the saturation magnetization and anisotropy constants. The latter are often expressed as an effective anisotropy constant K_{eff} , with contributions from bulk (magneto-crystalline), shape, surface, and strain.¹ Experimentally, K_{eff} is obtained from the coercive field, Mössbauer spectra, and ac magnetic susceptibility. In general, separation of K_{eff} into its different components is impossible to be performed, being the discussion centered in comparing K_{eff} to the value of bulk anisotropy. In the best case, K_{eff} is evaluated for a set of samples where the nanoparticles have different average volume in order to address changes in K_{eff} to changes in surface to volume ratio.² This approach is limited by the possibility of having systems with different average volumes keeping other parameters, e.g., interparticle distance and degree of crystallization, sufficiently well controlled. Ideally, separation of K_{eff} into its different components should be performed in one given system. In this letter we show that applied pressure induces structural and magnetic changes on maghemite ($\gamma\text{-Fe}_2\text{O}_3$) magnetic nanoparticles dispersed in a polymer that can be used to gain insight on the origin of anisotropy and to separate it into volume and surface contributions.

The maghemite/polymer nanocomposite used in the study here reported was prepared by the mixture of poly(vinylpyridine) (PVP) and iron bromide solution, followed by the precipitation of the nanoparticles induced by the addition of a base.³ The nanoparticles size at ambient pressure was estimated by transmission electron microscopy (TEM) as $D_0=5.1 \pm 0.5$ nm.⁴ The content of maghemite in mass is 16.4%. ac magnetic measurements of the nanocomposite were performed using a superconducting quantum interference device (SQUID) magnetometer (Quantum Design,

MPMS-5S). Pressurization and sample preparation were performed in accordance to Ref. 5 and the applied pressure was estimated by the shift of the superconducting transition temperature of Sn.⁶ Synchrotron radiation powder x-ray diffraction (XRD) measurements were performed at room temperature and pressures up to 27.7 kbar using a cylindrical imaging plate diffractometer (Rigaku Co.) at the Photon Factory (PF) of the Institute of Materials Structure Science, the High Energy Accelerator Research Organization (KEK), with $\lambda=0.6883(1)$ Å.⁷ Pressurization was performed by the use of a diamond anvil cell and a 0.3 mm thick Cu-Be gasket was inserted between the anvils. The sample and a few ruby crystals were held in a 0.4 mm hole located in the center of the gasket with the aid of a pressure-transmitting medium, fluorine oil (FC77). The pressure value was calibrated by the ruby fluorescence method.⁸ XRD and ac susceptibility measurements were performed for increasing pressure from ambient pressure to the maximum one. After releasing the maximum pressure, the reproducibility of the ambient pressure results was confirmed.

In the context of magnetic nanoparticles, superparamagnetism is one of the most interesting finite-size effects. In brief, by reducing size, the particle approaches the monodomain, behaving approximately as a single spin in a given energy landscape.¹ Below a given temperature and for a characteristic observation time, the single spin (nanoparticle magnetic moment) is not able to overcome the energy barriers ΔE and, in an ac magnetic susceptibility experiment, an out-of-phase component χ'' arises. ΔE is expressed as $K_{\text{eff}}V$, where V is the average nanoparticle volume. More generally, ΔE can be written as $\Delta E \propto V^p$,⁹ or as the sum of its different components $\Delta E=K_VV+K_S S+\dots$.¹ χ'' is related to the distribution of ΔE , $g(\Delta E)$, being in a first approach given by $\chi''(f, T) \propto \Delta E g(\Delta E)$, where f is the frequency of the ac field.^{10,11} The maximum T_B of $\chi''(T)$ of the maghemite nanoparticles (Fig. 1) presents a frequency dependence that can be described by the Néel–Arrhenius relation

$$\tau_m = \tau_0 \exp(\Delta E/k_B T_B), \quad (1)$$

where τ_0 is a microscopic characteristic time and τ_m is the characteristic measurement time equal to $1/(2\pi f)$. Equation

^{a)}Electronic mail: g586402y@tobata.isc.kyutech.ac.jp.

^{b)}Electronic mail: nunojoao@unizar.es.

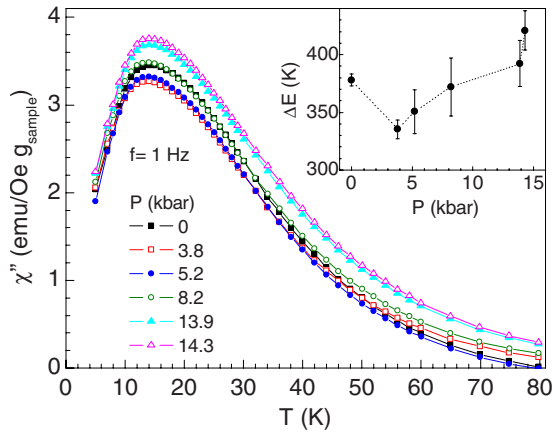


FIG. 1. (Color online) Out-of-phase component of the ac magnetic susceptibility χ'' for $f=1$ Hz and selected pressures P in the 0–14.3 kbar range. Inset shows the dependence of ΔE with pressure.

(1) is valid for negligible interparticle interactions. The existence of such interactions does not change the linear relation between $\ln(\tau_m)$ and $1/T_B$ (Arrhenius plot) but implies a change in ΔE and a decrease of the extrapolated τ_0 down to unphysical values.¹² For negligible interparticle interactions τ_0 in maghemite nanoparticles is of the order of 10^{-10} s, decreasing dramatically down to values of the order of 10^{-17} s and less as interactions become important.¹² In the present case, the extrapolated τ_0 is of the order of 10^{-11} s, changing less than one order of magnitude with pressure (which is of the order of the error bar). Therefore interactions are weak and Eq. (1) can be applied to estimate ΔE associated to a noninteracting nanoparticle and its change with pressure can be addressed to intraparticle effects. T_B derived from $\chi''(T)$ taken at $f=1$, 10, and 100 Hz has a small but apparent nonmonotonic change with pressure, decreasing and then increasing with pressure. Similar trend is displayed by ΔE (Fig. 1, inset), with ΔE being calculated based on Eq. (1) (using an Arrhenius plot). A nonmonotonic change with pressure has also been reported in magnetization experiments under a dc field performed in a maghemite/PVP nanocomposite with $D_0=6.5$ nm.¹³

Better insight on the structural origin of $\Delta E(P)$ is obtained by analyzing XRD patterns at different pressures. The diffraction pattern at ambient pressure shows broad peaks typical of nanosized materials at the positions expected for maghemite with a space group $P4_332$ (Ref. 14) and a background due to both the diamond anvils and the PVP matrix (Fig. 2).³ As pressure increases, both the peak positions and their shape change. In order to have a quantitative analysis, we have focused our attention on the most intense peak (with center around $2\theta=15^\circ$). For the XRD patterns at different pressures after subtracting the background, the region between 12° and 18° has a convolution of peaks that has been fitted to a sum of Lorentzians (Fig. 3), and the peak position and the full width at half maximum (FWHM) β determined. Pseudo-Voigt functions would be the choice given the peak broadening/shape induced by the instrument and nanoparticles, as it is apparent in similar nanocomposites where the maghemite nanoparticles have larger size and thus the XRD peaks are better defined. In the present case the peaks are broad and convoluted being important to decrease the number of parameters to guarantee the fit stability. We have chosen Lorentzian functions since the pseudo-Voigts above men-

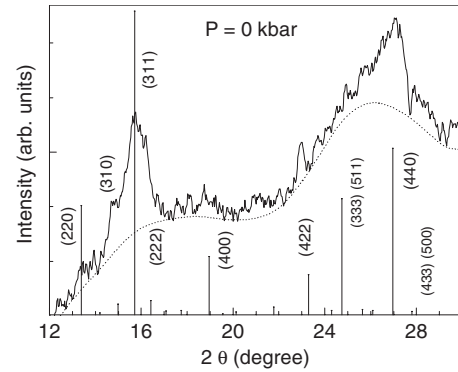


FIG. 2. XRD diffraction pattern of the maghemite/polymer nanocomposite at ambient pressure (solid line), background from pressure cell and polymer (dotted line) and expected positions for the diffraction peaks (Ref. 14) and associated planes.

tioned have higher Lorentzian character. In fact, Lorentzian fits give better agreement than Gaussian ones. The peak position and the FWHM can be associated to two different characteristic sizes (and then volumes, considering spherical nanoparticles) having their own pressure dependence as follows. On one hand, β can be associated to a coherence length D_{core} estimated from the Sherrer's formula as $D_{\text{core}}=0.9\lambda/(\beta \cos \theta)$. D_{core} has a nonmonotonic dependence with pressure resembling that of ΔE (Fig. 4). We have chosen to term the coherence length as D_{core} in the frame of a model where the region of the nanoparticle which diffracts coherently is associated to a core and any possible noncoherently diffracting region is associated to the surface. In fact, at ambient pressure D_{core} is smaller than D_0 estimated from TEM, the difference being of the order of 1 nm (Fig. 4) in accordance to the magnetic core-shell model proposed for similar maghemite nanocomposites, where shell thickness is 1 nm

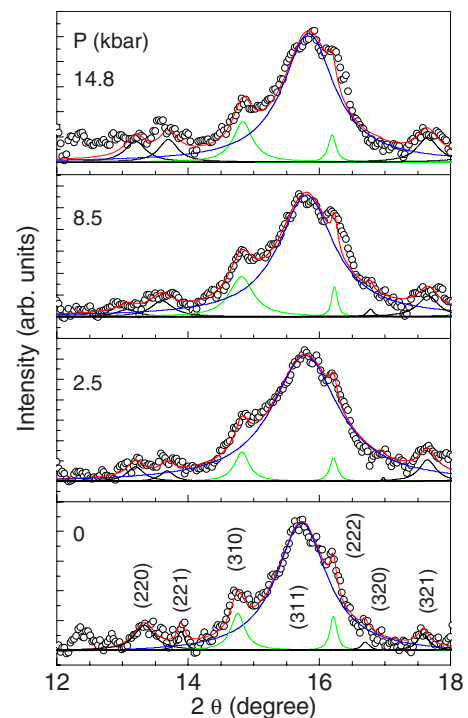


FIG. 3. (Color online) XRD diffraction pattern of the maghemite/polymer nanocomposite at selected pressures after subtracting background (open symbols), sum of the fitted Lorentzians and individual fitted Lorentzian curves.

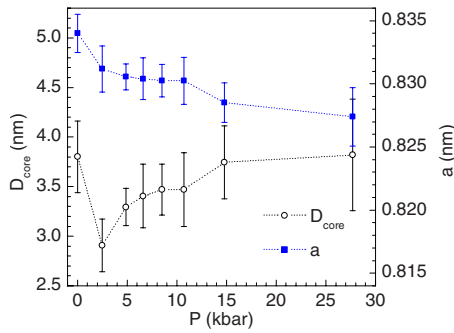


FIG. 4. (Color online) Cell parameter a and core diameter D_{core} as a function of pressure.

and constant in the 2–15 nm D_0 range.¹⁵ On the other hand, from the peak position a cell parameter a as a function of pressure is readily obtained (Fig. 4). The pressure dependence of the average nanoparticles volume is then proportional to the cell volume a^3 ,

$$V(P) = (\pi/6)D_0^3[a(P)/a_0]^3, \quad (2)$$

where a_0 is the cell parameter at ambient pressure.

By combining the information on $\Delta E(P)$ (Fig. 1, inset), $V_{\text{core}}(P) = (\pi/6)D_{\text{core}}^3(P)$ [with $D_{\text{core}}(P)$ from Fig. 4] and $V(P)$ as calculated from Eq. (2), we can eliminate the parameter pressure and analyze the core and total volume dependence of ΔE . In Fig. 5 it becomes apparent that while there is no simple relation between ΔE and V , ΔE is proportional to V_{core} . At the same time, for V_{core} equal to zero ΔE does not extrapolates to zero. This means that part of the anisotropy energy is due to the region of the nanoparticle that diffracts coherently, being proportional to the volume defined by that region, and part of the anisotropy is associated to the noncoherently diffracting region. In other words, the results shown in Fig. 5 suggest that the core-shell model is a good description for ΔE of the maghemite nanoparticles here studied. In this model, the linear relation between ΔE and V_{core} is expressed as

$$\Delta E = K_{\text{core}}V_{\text{core}} + K_S S, \quad (3)$$

yielding $K_{\text{core}} = 7.7 \times 10^5 \text{ erg/cm}^3$ and $K_S = 4.2 \times 10^{-2} \text{ erg/cm}^2$ considering the surface of a 5.1 nm diameter nanoparticle. In maghemite, the first order magnetocrystalline anisotropy constant K_1 is approximately -2.5

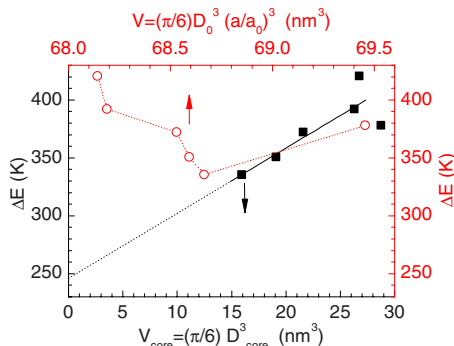


FIG. 5. (Color online) Magnetic anisotropy energy ΔE as a function of the average nanoparticles volume V (proportional to cube of the cell parameter a , open circles, top scale) and ΔE as a function of the nanoparticles core volume V_{core} (proportional to D_{core}^3 , squares, bottom scale). Solid line represents best linear fit to $\Delta E(V_{\text{core}})$ [Eq. (3)] and dotted line its extrapolation for $V_{\text{core}} = 0$.

$\times 10^5 \text{ erg/cm}^3$ and so, considering the easy axis to be (111) and the second order magnetocrystalline anisotropy constant K_2 negligible,¹⁶ the contribution of magnetocrystalline anisotropy to K_{eff} is of the order of $-K_1/12 = 2 \times 10^4 \text{ erg/cm}^3$. The value of K_{core} is therefore between that expected from the magnetocrystalline anisotropy and that usually found in maghemite nanoparticles ($3.6 - 6 \times 10^6 \text{ erg/cm}^3$).¹⁷ On the other hand, K_S is similar to that previously found for maghemite nanoparticles [$6 \times 10^{-2} \text{ erg/cm}^2$ (Ref. 18) and $4.2 \times 10^{-2} \text{ erg/cm}^2$ (Ref. 12)], and about one order of magnitude lower than that found in Co nanoparticles [$(2 - 3) \times 10^{-1} \text{ erg/cm}^2$] (Ref. 2) after analyzing K_{eff} for nanoparticles with different sizes. In view of this discussion, K_{eff} has a core component K_{core} whose origin is mainly magnetocrystalline anisotropy and an enhancement due to surface anisotropy. The clear separation between these components using only one system is possible since by applying pressure the ratio between the total nanoparticle volume and the coherently diffracting volume changes, leading to a change in the ratio between K_{core} and K_S .

The authors are grateful to M. A. Laguna and A. Larrea for their help with TEM and E. Lythgoe for critical reading of the manuscript. The work in Zaragoza has been supported by Grant No. MAT2007-61621 and CONSOLIDER-INGENIO 2010 Programme Grant No. CSD2007/0010 from the Ministry of Education.

¹J. L. Dormann, D. Fiorani, and E. Tronc, *Advances in Chemical Physics* (Wiley, New York, 1997), Vol. 98.

²F. Luis, J. M. Torres, L. M. García, J. Bartolomé, J. Stankiewicz, F. Petroff, F. Fettar, J. L. Maurice, and A. Vaurès, *Phys. Rev. B* **65**, 094409 (2002).

³A. Millan, F. Palacio, A. Falqui, E. Snoeck, V. Serin, A. Bhattacharjee, V. Ksenofontov, P. Gülich, and I. Gilbert, *Acta Mater.* **55**, 2201 (2007).

⁴See EPAPS Document No. E-APPLAB-94-014919 for a typical TEM micrograph of the nanocomposite and diameter distribution. For more information on EPAPS, see <http://www.aip.org/pubserv/epaps.html>.

⁵M. Mito, *J. Phys. Soc. Jpn. Suppl. A* **76**, 182 (2007).

⁶L. D. Jennings and C. A. Swenson, *Phys. Rev.* **112**, 31 (1958).

⁷A. Fujiwara, K. Ishii, T. Watanuki, H. Nakao, K. Ohwada, Y. Fujii, Y. Murakami, T. Mori, H. Kawada, T. Kikegawa, O. Shimomura, T. Matsubara, H. Hanabusa, S. Daicho, S. Kitamura, and C. Katayama, *J. Appl. Crystallogr.* **33**, 1241 (2000).

⁸G. J. Piermarini, S. Block, J. D. Barnett, and R. A. Forman, *J. Appl. Phys.* **46**, 2774 (1975).

⁹N. J. O. Silva, V. S. Amaral, L. D. Carlos, B. Rodríguez-González, L. M. Liz-Marzán, T. S. Berquó, S. K. Banerjee, V. de Zea Bermudez, A. Millán, and F. Palacio, *Phys. Rev. B* **77**, 134426 (2008).

¹⁰L. Lundgren, P. Svedlindh, and O. Beckman, *J. Magn. Magn. Mater.* **25**, 33 (1981).

¹¹T. Jonsson, J. Mattsson, P. Nordblad, and P. Svedlindh, *J. Magn. Magn. Mater.* **168**, 269 (1997).

¹²J. L. Dormann, F. D'Orazio, F. Lucari, E. Tronc, P. Prené, J. P. Jolivet, D. Fiorani, R. Cherkaoui, and M. Noguès, *Phys. Rev. B* **53**, 14291 (1996).

¹³Y. Komorida, M. Mito, H. Deguchi, S. Takagi, A. Millan, and F. Palacio, *J. Magn. Magn. Mater.* **310**, e800 (2007).

¹⁴A. N. Shmakov, G. N. Kryukova, S. V. Tsybulya, A. L. Chuvilin, and L. P. Solovyeva, *J. Appl. Crystallogr.* **28**, 141 (1995).

¹⁵A. Millan, A. Urtizberea, F. Palacio, N. J. O. Silva, V. S. Amaral, E. Snoeck, and V. Serin, *J. Magn. Magn. Mater.* **312**, L5 (2007).

¹⁶E. P. Valstyn, J. P. Hanton, and A. H. Morrish, *Phys. Rev.* **128**, 2078 (1962).

¹⁷B. Martínez, A. Roig, E. Molins, T. González-Carreño, and C. J. Serna, *J. Appl. Phys.* **83**, 3256 (1998).

¹⁸E. Tronc, A. Ezzir, R. Cherkaoui, C. Chanéac, M. Noguès, H. Kachkachi, D. Fiorani, A. M. Testa, J. M. Grenèche, and J. P. Jolivet, *J. Magn. Magn. Mater.* **221**, 63 (2000).